Uncoupling protein 3 expression and intramyocellular lipid accumulation by NMR following local burn trauma

QUNHAO ZHANG[1], HAIHUI CAO[1,2], LOUKAS G. ASTRAKAS[1,2], DIONYSSIOS MINTZOPOULOS[1,2], MICHAEL N. MINDRINOS[3], JOHN SCHULZ III[1], RONALD G. TOMPKINS[1], LAURENCE G. RAHME[1] and A. ARIA TZIKA[1,2]

[1]Department of Surgery, Massachusetts General Hospital, Shriners Burn Institute and Harvard Medical School; [2]Athinoula A. Martinos Center of Biomedical Imaging, Department of Radiology, Massachusetts General Hospital, Boston, MA 02114; [3]Department of Biochemistry, Stanford University School of Medicine, Stanford, CA 94305, USA

Received August 11, 2006; Accepted September 15, 2006

Abstract. Burn trauma is a clinical condition accompanied by muscle wasting that severely impedes rehabilitation in burn survivors. Mitochondrial uncoupling protein 3 (UCP3) is uniformly expressed in myoskeletal mitochondria and its expression has been found to increase in other clinical syndromes that, like burn trauma, are associated with muscle wasting (e.g., starvation, fasting, cancer, sepsis). The aim of this study was to explore the effects of burn trauma on UCP3 expression, intramyocellular lipids, and plasma-free fatty acids. Mice were studied at 6 h, 1 d and 3 d after nonlethal hindlimb burn trauma. Intramyocellular lipids in hindlimb skeletal muscle samples collected from burned and normal mice were measured using ^{1}H NMR spectroscopy on a Bruker 14.1 Tesla spectrometer at 4˚C. UCP3 mRNA and protein levels were also measured in these samples. Plasma-free fatty acids were measured in burned and normal mice. Local burn trauma was found to result in: 1) upregulation of UCP3 mRNA and protein expression in hindlimb myoskeletal mitochondria by 6 h postburn; 2) increased intramyocellular lipids; and 3) increased plasma-free fatty acids. Our findings show that the increase in UCP3 after burn trauma may be linked to burn-induced alterations in lipid metabolism. Such a link could reveal novel insights into how processes related to energy metabolism are controlled in burn and suggest that induction of UCP3 by burn in skeletal muscle is protective by either activating cellular redox signaling and/or mitochondrial uncoupling.

Correspondence to: Dr A. Aria Tzika, NMR Surgical Laboratory, Department of Surgery, Massachusetts General Hospital, Harvard Medical School, 51 Blossom Street, Room 261, Boston, MA 02114, USA
E-mail: atzika@partners.org or atzika@hms.harvard.edu

Key words: nuclear magnetic resonance, skeletal muscle, burn trauma, uncoupling protein 3, intramyocellular lipids

Introduction

Local burn trauma to skeletal muscle produces a pathophysiologic response (1,2) similar to that caused by other types of trauma. Although each type of traumatic insult can trigger myocellular dysfunction via a distinct extracellular stimulus, all insults are capable of producing a single common myocyte lesion (3). It has been suggested that the members of the uncoupling protein (UCP) family that may function by uncoupling oxidative phophorylation from ATP synthesis (4) are likely involved in a growing list of pathogenic conditions, including hyperthyroidism, cancer cachexia, diabetes, obesity and sepsis (5-8). To date, the molecular mechanisms involved in physiologic changes in skeletal muscle as a result of burn trauma, and in muscle wasting generally, remain uncertain.

UCP3 is a member of the mitochondrial UCP family expressed predominantly in the skeletal muscle of rodents and humans (9). Its role in normal physiology is not known, although this protein is hypothesized to be clinically relevant in pathophysiology (6,7,10,11). Studies in rodents indicate that UCP3 is not involved in thermoregulation, and that its uncoupling activity might, in fact, be a consequence of some as yet unknown primary function (4,10,12,13). The observation that UCP3 expression is increased in situations where fatty acid (FA) entry into the mitochondria exceeds ß-oxidation capacity suggests that this protein may be involved in the outward translocation of FA from the mitochondrial matrix. This translocation would prevent a deleterious intramitochondrial accumulation of FA (14,15). Consistent with the hypothesis that UCP3 is involved in FA transport, UCP3 mRNA expression has been found to be dramatically increased in humans who fast (16) and this phenomenon was found to be mediated by increased levels of circulating free FA (FFA) (17). In obese humans, a positive correlation was observed between the level of circulating FFA and muscle UCP3 mRNA expression (18). Furthermore, in humans, an increased level of circulating FFA induced by lipid infusion stimulated UCP3 mRNA expression in muscle (19). These experiments indicate a pivotal role of FA in the control of UCP3 mRNA expression. Other experiments have demonstrated a direct relationship between FFA and UCP3 mRNA expression (20,21). It has

also been suggested that increased expression of UCP3 under conditions of increased FA metabolism implies an as yet unidentified role in lipid metabolism (10).

NMR is a biochemistry-based method used for evaluation of skeletal muscle (22-24) and has been used in burn trauma studies (25-27). The NMR technique employed herein, high-resolution magic angle spinning (HRMAS) ^{1}H NMR spectroscopy, a technique used for solids, can produce high-resolution spectra for intact biological samples (28). Compared to conventional high-resolution *in vitro* NMR of tissue extracts, *ex vivo* HRMAS ^{1}H NMR of intact tissues not only yields superior biochemical information, but sample preparation is simplified and the *in vivo* state is better approximated (29). This technique is being used increasingly to investigate overt cellular diseases (30-32). To identify metabolic and molecular aberrations associated with burn trauma, we applied high-resolution HRMAS ^{1}H NMR to intact *ex vivo* muscle samples from animals subjected to burn trauma. The changes observed might also reflect aberrations in lipid metabolism, as some of the peaks detected by HRMAS ^{1}H NMR in skeletal muscle arise from intramyocellular lipids (IMCLs) (22).

We used a mouse model to study UCP3 expression following a local burn in the animal's hindlimb, which has been well characterized (33,34). An increase in mitochondrial UCP3 expression in the animal's hindlimb muscle concomitant with accumulated IMCLs would be consistent with the hypothesis that UCP3 upregulation is linked to burn-induced aberrant lipid metabolism. For purposes of our study, we measured the level of expression of UCP3 mRNA and protein, and the levels of IMCLs and plasma-free fatty acids in the hindlimbs of two experimental groups: mice that had sustained local hindlimb burn injury and healthy unburned mice serving as controls.

Materials and methods

Experimental animals. Male, 6-week-old CD1 mice weighing ~20-25g were purchased from Charles River Laboratory (Boston, MA). The animals were maintained on a regular light-dark cycle (light on from 8 a.m. to 8 p.m.) at an ambient temperature of 22±1˚C; they had free access to food and water.

The mouse burn model employed was a local hindlimb burn of ~3-5% TBSA. The left hindlimb muscle was harvested at selected times following burn injury to examine changes in whole muscle gene expression.

All animal experiments were approved by the Subcommittee on Research Animal Care of the Massachusetts General Hospital, Boston, MA.

Hindlimb burn (local burn model). Prior to receiving burn injury, mice were anesthetized by intraperitoneal injection of 40 mg/kg pentobarbital sodium and were randomized into burn or control groups.

The left hindlimb of all mice in both groups (control and burn) was shaved and each mouse in the burn group (n=6) was subjected to a nonlethal scald injury of 3-5% body surface area by immersion of the left hindlimb in 90˚C water for 3 sec. This method has been previously established (33) and is thought to be a clinically relevant model of common burn injuries based on the tissue temperature (between soleus muscle and fibula) reaching 46-54˚C, similar to the temperature at which human tissue shows thermal damage. After injury, animals were given analgesia in the form of buprenorphine 0.05-0.1 mg/kg SQ, as required.

Gastrocnemius muscle was used for analysis in all cases because it has previously been shown that effectors of UCP3 expression, such as fasting and high-fat feeding, exert a more pronounced effect in fast-twitch glycolytic (white) muscle, and responses to injury would thus be easier to detect.

System control: TNF-α administration. TNF-α has been shown to evoke an increase in UCP3 expression in muscle mitochondria. Consequently, we used TNF-α challenge as a system control. Mice were randomly divided into TNF-α (Sigma, St. Louis, MO, USA) treated and saline control groups. Experimental mice were injected intraperitoneally with a single dose of TNF-α (100 μg/kg body weight in 0.5 ml of saline). Control mice were injected intraperitoneally with 0.5 ml of saline. After administration (12, 24 or 96 h) of TNF-α (or saline control), mice were anesthetized as described above and gastrocnemius muscle from TNF-α treated and control animals was excised, placed immediately in ice-cold buffer and then used for mitochondrial isolation.

Mitochondria isolation. All procedures were performed at 4˚C unless otherwise specified. Mitochondrial proteins were isolated from mouse gastrocnemius muscle immediately after excision. Muscle tissue was finely minced, then ground and homogenized in 10-20 ml of cold phosphate-buffered saline (137 mM NaCl, 3 mM KCl, 6.5 mM Na_2HPO_4, pH 7.2) with 1% protease inhibitor cocktail (Sigma) and kept on ice. Homogenate was centrifuged at 600 x g for 10 min at 4˚C. The pellet was discarded, and the supernatant was transferred to a fresh tube. Mitochondrial protein concentrations were determined as described by Bradford using the Bio-Rad protein assay, with BSA as a standard. The isolated mitochondria were stored at -20˚C, awaiting Western blot analysis.

Western blot analysis. Affinity-purified rabbit anti-Rat UCP3 was purchased from Alpha Diagnostic International (San Antonio, TX, USA), website: www.4adi.com. Since mouse and rat UCP3 are identical, the antibody can be used as a probe in both species. Mitochrondrial proteins (50 μg) were separated by SDS-polyacrylamide gel electrophoresis (4-15% Tris-HCl gel; Bio-Rad) and transferred to a nitrocellulose membrane (Bio-Rad). The nitrocellulose membrane was blocked in a buffer containing 5% milk in 1X TBS and 0.1% Tween-20 for 1 h at room temperature. The membrane was incubated with UCP3 antibody as primary antibody (5:1000 dilution) at 4˚C overnight. The membrane was washed 6 times (each wash 5-10 min) in 0.1% Tween-20 and 1X TBS (wash buffer) at 4˚C and then incubated with goat anti-rabbit IgG-horseradish peroxidase conjugate (1:10,000) for 1 h at room temperature. The membrane was then washed 6x10 min in wash buffer and exposed with ECL to hyperfilm. Bands were quantified by densitometry scanning (Amersham Pharmacia Biotech, website: www.amershambiosciences.com). Blots were probed with rabbit monoclonal anti-actin antibody (Sigma) as an internal standard. The molecular weight of the proteins was assessed by using protein molecular mass standards (Bio-Rad).

After quantitation, the results were expressed as arbitrary units based on UCP3/actin densitometric ratios.

Extraction of RNA. At each time point of 6, 24, and 72 h postburn, 4 burned and 4 control mice were anesthetized by intraperitoneal injection of 40 mg/kg pentobarbital and the gastrocnemius was excised.

All mice were then administered a lethal dose of pentobarbital (200 mg/kg) IP. The muscle was immediately immersed in 1 ml TRizol (Invitrogen, Carlsbad, CA, USA) for RNA isolation. The muscle was homogenized for 60 sec using a Brinkman Polytron 3000 before extraction of total RNA. Chloroform (200 μl) was added to the homogenized muscle and mixed by inverting the tube for 15 sec. After centrifugation at 12000 g for 15 min, the upper aqueous phase was collected and precipitated by adding 500 μl isopropanol. Further centrifugation at 12,000 g for 10 min separated the RNA pellet, which was then washed with 500 μl 70% ethanol and centrifuged at 7,500 g for 5 min prior to air-drying. The pellet was resuspended in 100 μl DEPC-H20. RNeasy kit (Qiagen, MD, USA) was used to purify the RNA according to the manufacturer's protocol. Purified RNA was quantitated by UV absorbance at 260 and 280 nm and stored at -70˚C for DNA microarray analysis.

Microarray hybridization. Biotinylated cRNA was generated with 10 μg of total cellular RNA according to the protocol outlined by Affymetrix Inc. (Santa Clara, CA, USA). cRNA was hybridized onto MOE430A oligonucleotide arrays (Affymetrix), stained, and washed and scanned according to Affymetrix protocol.

Genomic data analysis. The data files of scanned image files hybridized with probes from RNA extracted from gastrocnemius isolated at the specified times from burned or unburned control mice (n=2) were converted to cell intensity files (CEL files) with the Microarray suite 5.0 (MAS, Affymetrix). The data were scaled to target intensity of 500, and for each time point all possible pairwise array comparisons of the replicates to normal control mice were performed (i.e., four combinations when two arrays from each time point were compared to the two arrays hybridized to RNA from control mice), using a MAS 5.0 change call algorithm. Probe sets that had a signal value difference >100 and in which one of the two samples being compared was not called 'Absent' in each comparison, were scored as differentially modulated when 1) the number of change calls in the same direction were at least 3, 4, and 6 when the number of comparisons were 4, 6 and 9, respectively; and 2) the other comparisons were unchanged. Such scoring is to partially compensate for biological stochasticity and technical variation. Based on the ratios of 100 genes determined to be invariant in most conditions tested (Affymetrix) in the hindlimb burn and control animals, an additional constraint of a minimum ratio of 1.65 was applied to control the known false positives at 5% hindlimb.

^{1}H NMR spectroscopy. Hindlimb skeletal muscle samples collected from burned and control mice were measured using high-resolution magic angle spinning (HRMAS) ^{1}H NMR spectroscopy on a Bruker 14.1 Tesla spectrometer at 4˚C. The Carr-Purcell-Meiboom-Gill (CPMG) spin-echo pulse sequence with a total spin-spin relaxation delay of 10 ms was used to measure spin-echo HRMAS ^{1}H NMR spectra on all samples. Typically, 256 transients were collected into 32 K data points. The number of 180 degree cycles was n=2. The MestRe-C NMR software package (Mestrelab Research, NMR solutions, website: www.mestrec.com) was used for peak quantification. Free induction decays were zero filled and apodized with exponential multiplication (2 Hz) before Fourier transformation. The spectra were then manually phased, corrected for broad baseline features and curve-fitted using Lorentzian and Gaussian functions. The Kolmogorov-Smirnov test and Levene's test were used to assess normality of the variables and homogeneity of variances, respectively. Analysis of variance (ANOVA) was also performed by using parametric and nonparametric methods to ensure that differences or lack of differences between groups was consistent. The differences in the 1.4 PPM peak to total creatine ratio (IMCLs) were evaluated by using the nonparametric Kruskal-Wallis test. Pearson product moment correlation coefficient (r) was used to assess the strength of association between IMCLs ratio and T2. Statistical analysis was conducted by using SPSS, version 12.0 (SPSS, Chicago, IL, USA). A two-tailed value of <0.05 was considered to indicate a statistically significant difference.

Plasma FFA assay. Blood was drawn by heart puncture at the time of sacrifice and plasma FFA level was measured by using the calorimetric FFA assay kit that uses acylation of coenzyme A (NEFA C; Wako Chemicals USA, Inc., Richmond, VA, USA). Results of the Kolmogorov-Smirnov test of normality indicated that no group significantly departed from a Gaussian distribution. Mean differences between the control group and burn groups were evaluated with unpaired t-tests (Table II). A two-tailed $P<0.05$ was considered statistically significant.

Results

Burn injury upregulates the UCP3 gene and protein expression in skeletal muscle. As part of a project to identify mitochondrial gene expression changes in skeletal muscle following burn, we carried out a transcriptome comparative analysis between burn and unburned animals at selected time points, using the Affymetrix GeneChip technology. The expression profiles show that from all UCP genes, present in the Affymetrix GeneChip MOE430A, only UCP3 gene expression is altered in skeletal muscle following burn. As shown in Fig. 1A, by 6 h post-burn UCP3 mRNA expression has increased, by 24 h, it returns close to normal levels, if not slightly lower, and at 3 d it appears to be further decreased. Results obtained with Western blot studies (Fig. 1B and C) demonstrate that burn trauma upregulates the 34 kDa UCP3 protein within 6 h. Samples at 6 h and 1 d postburn have increased levels of UCP3 protein versus samples from control animals or from experimental animals at 3 d postburn. The burn-induced 2-fold increase in mitochondrial UCP3 protein expression persists for at least 24 h after the injury in contrast to the more transient rise in UCP3 mRNA. By 3 d postburn, UCP3 protein

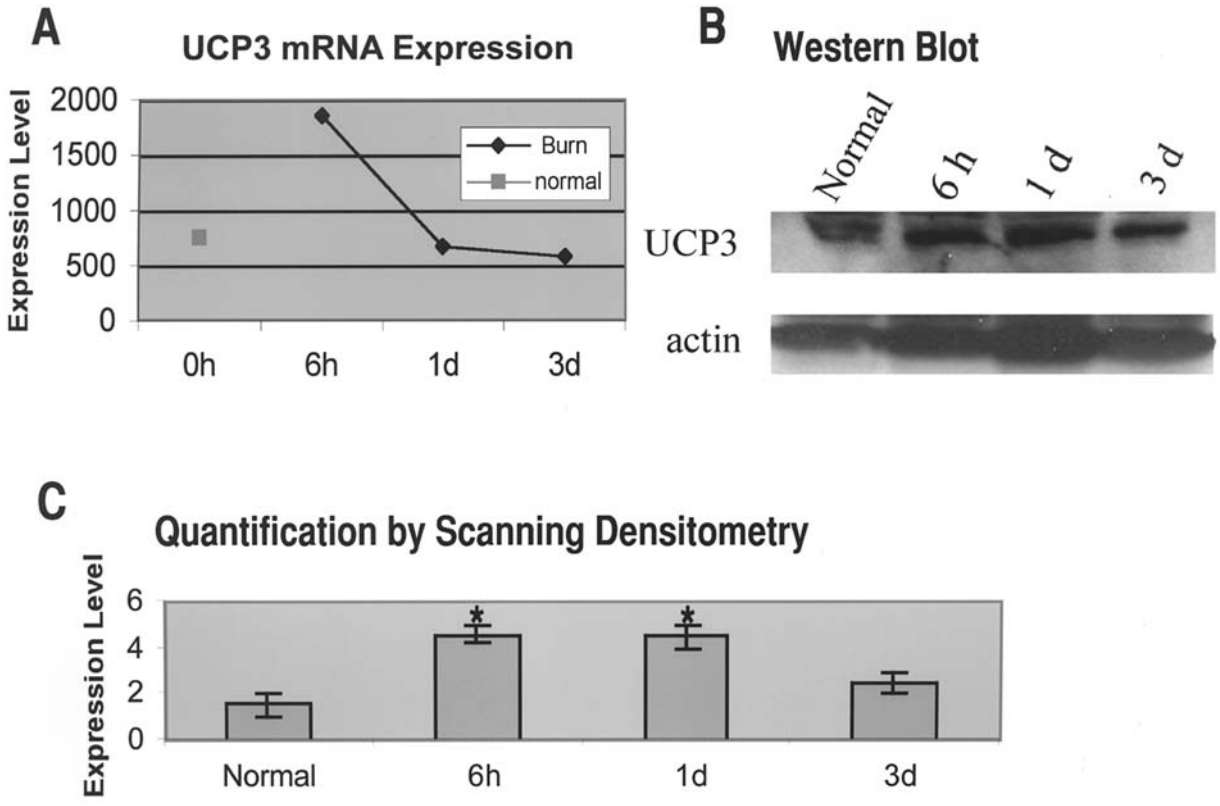

Figure 1. UCP3 expression after hindlimb burn. Expression levels of UCP3 in hindlimb skeletal muscle of normal (control) mice and of burned mice at 6 h, 1 d and 3 d postburn. UCP3 mRNA expression increases up to 6 h postburn and returns to normal levels by 24 h (A). Representative Western blots (B) and quantifications by densitometry (C) are shown. Western blot analysis of 50 μg mitochondria isolated from normal mice (normal, lane 1) or burned mice at 6 h, and 1 and 3 d postburn (lanes 2-4). Actin was used as internal control. Autoradiographs were quantified by scanning densitometry and results expressed as arbitrary units. Results are means ± SE, n=6 in each group. *P<0.05 between normal and postburn groups by Student's t-test.

Table I. Intramyocellular lipids and their T2 values following burn trauma.

	Normal (n=6)	6 h (n=6)	1 d (n=3)	3 d (n=3)	P01	P02	P03	P12	P13	P23
IMCLs	1.8±0.1[a]	2.4±0.1	8.3±0.6	9.1±0.5	0.01	0.02	0.01	0.02	0.01	NS
T2	87±11	105±7	86±3	96±13	0.02	NS	NS	NS	NS	NS

[a]Values are means ± SE and post hoc multiple comparisons. Normal, 6 h, 1 d and 3 d groups are assigned the group numbers 0, 1, 2, 3, respectively; thus, P13 indicates P-value for comparison of 1 and 3 group, i.e., between 6 h and 3 d. P-values shown have been obtained with Tukey's test for T2 and with the Games-Howell test for ratio variable. Other post hoc comparison tests confirm these results. IMCLs, intramyocellular lipids; NS, not significant.

expression has almost returned to preburn levels. UCP3 mRNA and protein expression from control animals did not change from baseline at any time point.

Although the UCP3 gene expression returns to normal by 24 h postburn (Fig. 1A), the increase in UCP3 protein expression is sustained for at least 24 h postburn (Fig. 1C). To determine whether the increased UCP3 protein level at 24 h postburn is due to its high stability, we used TNF-α, known to increase UCP3 gene expression in mice (35), to independently activate UCP3 (Fig. 2). UCP3 gene expression is known to peak by 12 h and return to normal levels by 24 h following TNF-α administration (35). As shown in Fig. 2, UCP3 protein levels are sustained for at least 24 h postTNF-α, indicating the high stability of the protein.

Burn trauma causes accumulation of intramyocellular lipids (IMCLs). Our HRMAS ^{1}H NMR spectra showed differences between muscle from burned and control animals at 1.4 ppm (Fig. 3, peak 2), exhibiting IMCLs that appear to increase after burn trauma (Fig. 3). Since the data for the IMCL variable were heavily skewed and failed to meet the assumption of homogeneity of variances, a natural logarithmic transformation was used to normalize them when needed. The Kolmogorov-Smirnov test of normality indicated that only T2 values

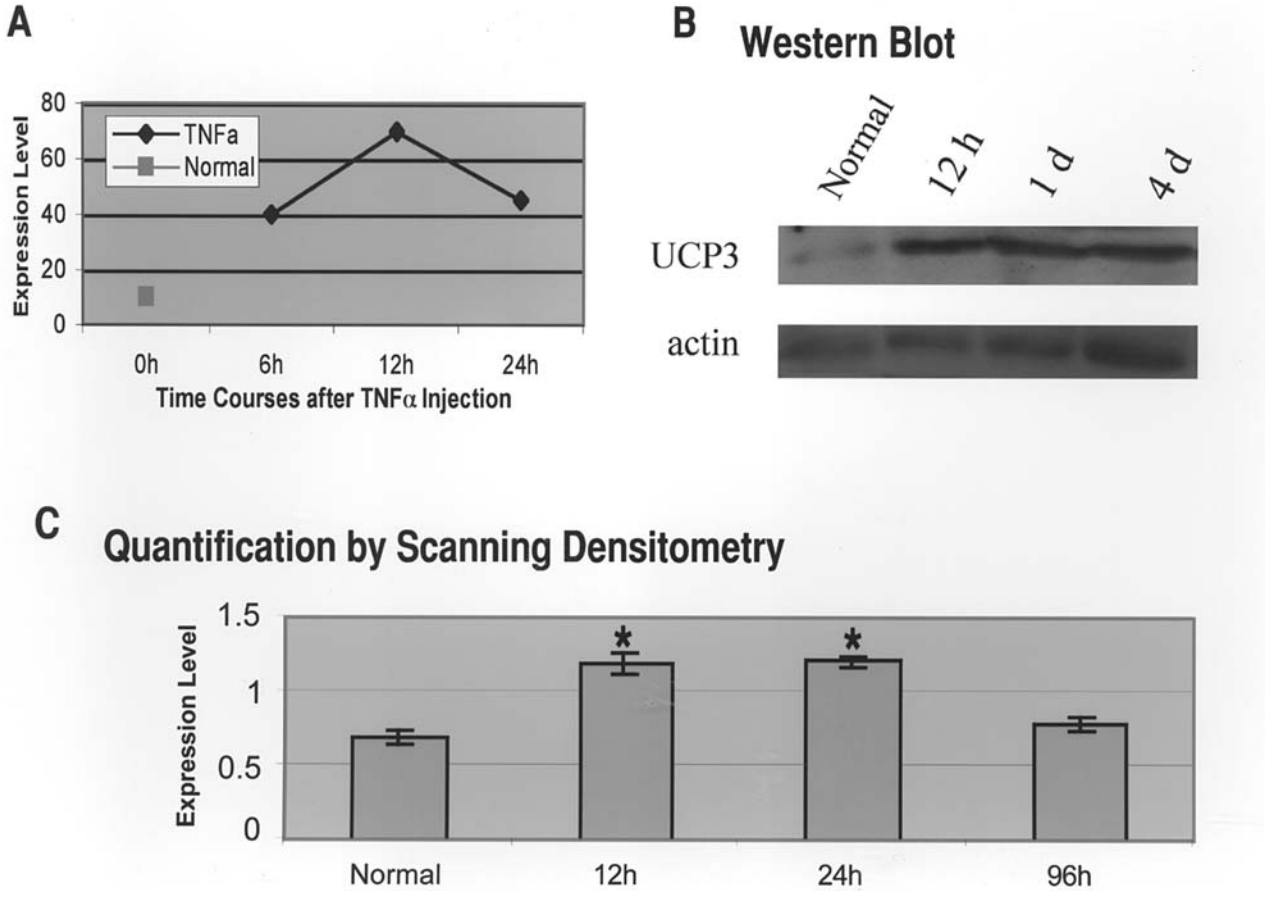

Figure 2. UCP3 expression after injecting TNF-α. Expression levels of UCP3 in hindlimb skeletal muscle of mice 12, 24 and 96 h after injecting a single dose of TNF-α (100 μg/kg body weight in 0.5 ml of saline) intraperitoneally; normal sham mice injected with 0.5 ml of saline. UCP3 mRNA expression (A), representative Western blots (B) and quantifications by densitometry (C) are shown. Actin was used as internal control. Autoradiographs were quantified by scanning densitometry and results expressed as arbitrary units. Results are means ± SE, n=6 in each group. *P<0.05 between normal and postburn groups by Student's t-test.

conformed to a normal distribution. Similarly Levene's test indicated that only T2 had the same variance in every time category.

T2 measurements did not correlate with the IMCL ratio (r=-0.12, P=0.62) or even with normalized ratio values (r=0.09, P=0.73). The Kruskal-Wallis test [df=3, P(T2)=0.03, P(ratio)=0.002] and ANOVA analysis [df=3, P(T2)=0.21, P(ratio)<0.001] demonstrated that time is significantly related both to T2 and ratio due to differences in their mean values in the four time groups. However, only the IMCL ratio variable: a) exhibited a significant trend with time (P<0.001) and b) was significantly different between control and burned animals (P<0.001). Post-hoc multiple comparisons between means of variables T2 and ratio for different time groups are shown in Table I. Again it appears that only the IMCL variable increased with time until the 1st day following burn.

Burn trauma increases plasma-free fatty acid (FFA) levels in the hindlimb burn model. Based on our data showing that burn trauma triggers an upregulation of UCP3 mRNA and protein in muscle, we investigated whether UCP3 upregulation coincides with an increase in plasma-free fatty acid levels in the hindlimb burn model. Table II shows FFA levels increase over the first 6 h postburn and remain significantly elevated through 72 h postburn (P<0.001; unpaired t-tests).

Discussion

The present study is the first to demonstrate that burn trauma also triggers an upregulation of UCP3 mRNA and protein in muscle, accompanied by an increase in plasma FFA that coincides with accumulation of IMCLs. The increase in UCP3 expression in skeletal muscle following local burn may be a protective mechanism involving mitochondrial uncoupling and prevention of apoptosis. Such a process appears to take place in experimental stroke studies where induction of UCP2 occurs (36). Failure in UCP3 induction or reduced UCP3 expression may lead to apoptosis as observed in burned skeletal muscle (37). Our findings suggest a more general role for UCP3, one that is implicated in a variety of traumatic situations.

A principal finding of our experiments is that burn trauma upregulates the 34 kDa UCP3 protein in the first 6 h postburn, and that the upregulation is sustained for at least 24 h postburn (Fig. 1C) although UCP3 mRNA expression returns to normal by 24 h. Our positive control experiments with TNF-α administration, which may mimic the effects of burn, since it

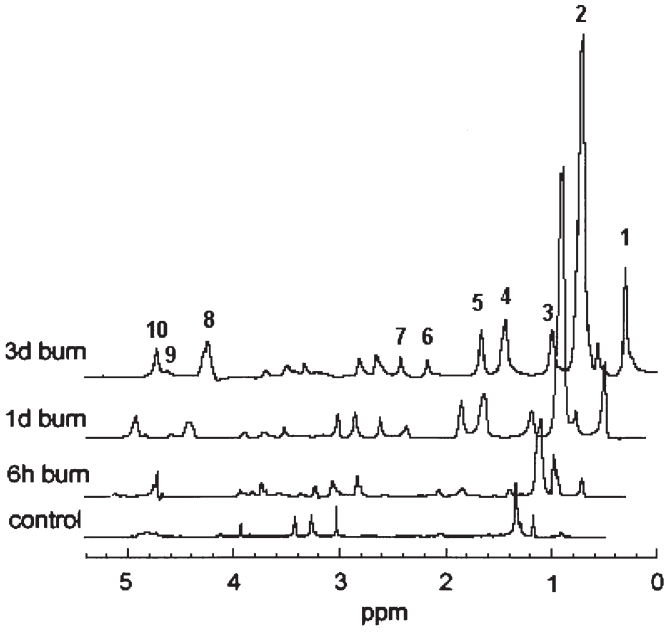

Figure 3. Water suppressed high-resolution magic angle spinning (HRMAS) ^{1}H NMR spectroscopy of skeletal muscle tissue following burn trauma. Peaks: 1, CH_3- lipids; 2, $(CH_2)_n$ lipids; 3, CH_2-CH_2-CO lipids; 4, CH = CH-CH_2-CH_2 lipids; 5, CH_2-CH_2-CO lipids; 6, = CH-CH_2-CH = lipids; 7, total creatine; 8, residual water; 9, = CH- lipids; 10, -CH = lipids. Lipids resonances (peaks 1-6, 9, 10) increase over time after burn. Peak 2, at 1.4 ppm, exhibits increase of IMCLs following burn trauma.

has been shown to increase following burn (38), showing that UCP3 protein levels are sustained for at least 24 h post TNF-α, (Fig. 2) demonstrate that the increased UCP3 protein level at 24 h post-burn is due to its high stability. Nevertheless, both mRNA and protein data, along with the NMR findings presented herein, suggest that UCP3 protein may promote the mitochondrial dysfunction that underlies the skeletal muscle wasting and general cachexia of burn pathophysiology (39). Whether UCP3 has a role in mitochondrial uncoupling in burn trauma needs to be investigated using *in vivo* assessment of mitochondrial energy coupling by NMR which is superior to electric potential measurements across the inner mitochondrial membrane (40).

Our results also demonstrated that the accumulation of mobile lipids in muscle tissue in response to burn trauma coincides with UCP3 upregulation. As shown in Fig. 3, the peak at 1.4 ppm, which has been attributed to methylene protons of intramyocellular triglyceride acyl chains, arising primarily as a result of increased IMCL (22), increases with advancing burn. This suggests that the increase in the peak at 1.4 ppm may be due primarily to an increase in IMCL as was visible by NMR. This suggestion is further supported by the results of previous studies in humans (41,42).

The results presented in Table II showing an increase in FFA levels by 6 h postburn and remaining significantly elevated through 72 h postburn are consistent with the notion of a link between increasing FFA and alterations in UCP3 expression, also found to rise by 6 h (Fig. 1). Various physiologic and pathologic states associated with raised UCP3 mRNA levels in skeletal muscle also show elevated plasma FFA levels, and our findings suggest that changes in FFAs

Table II. Plasma free fatty acids following burn trauma.

Group (n=6)	Plasma FFA[a]	P-values[b]
Normal	0.20±0.05[a]	-
6 h	0.28±0.06	0.038
12 h	0.35±0.07	<0.001
24 h	0.39±0.07	<0.001
72 h	0.43±0.05	<0.001

[a]Values are means ± SE. [b]T-test for equality of mean with the normal group.

might signal altered UCP3 expression. Understanding the link between FFAs and UCP3 expression could provide new information on how the processes related to energy metabolism are affected by burn trauma (43). It has been shown in rodents and humans that UCP3 expression in muscle is controlled by the levels of circulating and probably intramuscular FFA (17,19,20). The results of the present study suggest that a potential mechanism for decreased contractile function in burn trauma partially supported by our findings and the general understanding in burn trauma is as follows: burn causes increase in plasma FFA, increased delivery of FA to the skeletal muscle leading to activation of UCP3, insulin resistance (44) and thus decreased glucose uptake. Consequently, energy deficiency might result from increased UCP3 (i.e, less efficient ATP synthesis) and reduced glucose uptake. To correct these defects a treatment that would lower plasma FFA and simultaneously provide an alternative energy source may be proposed. To date, however, we have not established causal relationships linking IMCLs, UCP3 and FFA in our model; they all seem to rise 6 h after burn. Nevertheless, our results agree with the notion that UCP3 may have an as yet unidentified role in lipid metabolism (10).

We believe that our findings may have significant clinical implications. Not only is burn trauma in our mouse model comparable to common burn injuries in humans (33,34) but our findings may explain cellular changes brought about by thermal ablations associated with high-intensity focused ultrasound, increasingly used in treating a variety of inoperable cancers (45). Finally, these findings open a door to a better understanding of physiological and pathological processes attendant to local burn trauma and suggest further exploration of the role of UCP3 in a variety of traumatic situations which may be protective by either activating cellular redox signaling and/or mitochondrial uncoupling.

Acknowledgements

This work was supported in part by National Institutes of Health (NIH) Center Grant P50GM021700. Q.Z. was a Shriners Research Fellow.

References

1. Helm PA, Pandian G and Heck E: Neuromuscular problems in the burn patient: cause and prevention. Arch Phys Med Rehabil 66: 451-453, 1985.

2. Sheridan RL and Tompkins RG: What's new in burns and metabolism. J Am Coll Surg 198: 243-263, 2004.
3. Mitch WE and Goldberg AL: Mechanisms of muscle wasting. The role of the ubiquitin-proteasome pathway. N Engl J Med 335: 1897-1905, 1996.
4. Boss O, Muzzin P and Giacobino JP: The uncoupling proteins, a review. Eur J Endocrinol 139: 1-9, 1998.
5. Gong DW, He Y, Karas M and Reitman M: Uncoupling protein-3 is a mediator of thermogenesis regulated by thyroid hormone, beta3-adrenergic agonists, and leptin. J Biol Chem 272: 24129-24132, 1997.
6. Argiles JM, Busquets S and Lopez-Soriano FJ: The role of uncoupling proteins in pathophysiological states. Biochem Biophys Res Commun 293: 1145-1152, 2002.
7. Krauss S, Zhang CY and Lowell BB: The mitochondrial uncoupling-protein homologues. Nat Rev Mol Cell Biol 6: 248-261, 2005.
8. Sun X, Wray C, Tian X, Hasselgren PO and Lu J: Expression of uncoupling protein 3 is upregulated in skeletal muscle during sepsis. Am J Physiol Endocrinol Metab 285: E512-E520, 2003.
9. Boss O, Samec S, Paoloni-Giacobino A, *et al*: Uncoupling protein-3: a new member of the mitochondrial carrier family with tissue-specific expression. FEBS Lett 408: 39-42, 1997.
10. Nedergaard J and Cannon B: The 'novel' 'uncoupling' proteins UCP2 and UCP3: what do they really do? Pros and cons for suggested functions. Exp Physiol 88: 65-84, 2003.
11. Nedergaard J, Ricquier D and Kozak LP: Uncoupling proteins: current status and therapeutic prospects. EMBO Rep 6: 917-921, 2005.
12. Muzzin P, Boss O and Giacobino JP: Uncoupling protein 3: its possible biological role and mode of regulation in rodents and humans. J Bioenerg Biomembr 31: 467-473, 1999.
13. Boss O, Hagen T and Lowell BB: Uncoupling proteins 2 and 3: potential regulators of mitochondrial energy metabolism. Diabetes 49: 143-156, 2000.
14. Himms-Hagen J and Harper ME: Physiological role of UCP3 may be export of fatty acids from mitochondria when fatty acid oxidation predominates: an hypothesis. Exp Biol Med 226: 78-84, 2001.
15. Schrauwen P, Saris WH and Hesselink MK: An alternative function for human uncoupling protein 3: protection of mitochondria against accumulation of nonesterified fatty acids inside the mitochondrial matrix. FASEB J 15: 2497-2502, 2001.
16. Millet L, Vidal H, Andreelli F, *et al*: Increased uncoupling protein-2 and -3 mRNA expression during fasting in obese and lean humans. J Clin Invest 100: 2665-2670, 1997.
17. Weigle DS, Selfridge LE, Schwartz MW, *et al*: Elevated free fatty acids induce uncoupling protein 3 expression in muscle: a potential explanation for the effect of fasting. Diabetes 47: 298-302, 1998.
18. Boss O, Bobbioni-Harsch E, Assimacopoulos-Jeannet F, *et al*: Uncoupling protein-3 expression in skeletal muscle and free fatty acids in obesity. Lancet 351: 1933, 1998.
19. Khalfallah Y, Fages S, Laville M, Langin D and Vidal H: Regulation of uncoupling protein-2 and uncoupling protein-3 mRNA expression during lipid infusion in human skeletal muscle and subcutaneous adipose tissue. Diabetes 49: 25-31, 2000.
20. Samec S, Seydoux J and Dulloo AG: Skeletal muscle UCP3 and UCP2 gene expression in response to inhibition of free fatty acid flux through mitochondrial beta-oxidation. Pflugers Arch 438: 452-457, 1999.
21. Schrauwen P, Hinderling V, Hesselink MK, *et al*: Etomoxir-induced increase in UCP3 supports a role of uncoupling protein 3 as a mitochondrial fatty acid anion exporter. FASEB J 16: 1688-1690, 2002.
22. Szczepaniak LS, Babcock EE, Schick F, *et al*: Measurement of intracellular triglyceride stores by H spectroscopy: validation *in vivo*. Am J Physiol 276: E977-E989, 1999.
23. Vermathen P, Kreis R and Boesch C: Distribution of intramyocellular lipids in human calf muscles as determined by MR spectroscopic imaging. Magn Reson Med 51: 253-262, 2004.
24. Thomas MA, Chung HK, and Middlekauff H: Localized two-dimensional ^{1}H magnetic resonance exchange spectroscopy: a preliminary evaluation in human muscle. Magn Reson Med 53: 495-502, 2005.
25. Xia Z, Horton JW and Zhao P: NMR relaxation studies on hepatic intracellular and extracellular sodium in rats with burn injury. J Burn Care Rehabil 18: 193-199, 1997.
26. Yarmush DM, MacDonald AD, Foy BD, Berthiaume F, Tompkins RG, and Yarmush ML: Cutaneous burn injury alters relative tricarboxylic acid cycle fluxes in rat liver. J Burn Care Rehabil 20: 292-302, 1999.
27. Sikes PJ, Zhao P, Maass DL and Horton JW: Time course of myocardial sodium accumulation after burn trauma: a (31)P- and (23)Na-NMR study. J Appl Physiol 91: 2695-2702, 2001.
28. Cheng LL, Lean CL, Bogdanova A, *et al*: Enhanced resolution of proton NMR spectra of malignant lymph nodes using magic-angle spinning. Magn Reson Med 36: 653-658, 1996.
29. Cheng LL, Ma MJ, Becerra L, *et al*: Quantitative neuropathology by high resolution magic angle spinning proton magnetic resonance spectroscopy. Proc Natl Acad Sci USA 94: 6408-6413, 1997.
30. Morvan D, Demidem A, Papon J, De Latour M and Madelmont JC: Melanoma tumors acquire a new phospholipid metabolism phenotype under cystemustine as revealed by high-resolution magic angle spinning proton nuclear magnetic resonance spectroscopy of intact tumor samples. Cancer Res 62: 1890-1897, 2002.
31. Tzika AA, Cheng LL, Goumnerova L, *et al*: Biochemical characterization of pediatric brain tumors by using *in vivo* and *ex vivo* magnetic resonance spectroscopy. J Neurosurg 96: 1023-1031, 2002.
32. Cheng LL, Burns MA, Taylor JL, *et al*: Metabolic characterization of human prostate cancer with tissue magnetic resonance spectroscopy. Cancer Res 65: 3030-3034, 2005.
33. Tomera JF and Martyn J: Systemic effects of single hindlimb burn injury on skeletal muscle function and cyclic nucleotide levels in the murine model. Burns Incl Therm Inj 14: 210-219, 1988.
34. Shangraw RE and Turinsky J: Effect of disuse and thermal injury on protein turnover in skeletal muscle. J Surg Res 33: 345-355, 1982.
35. Busquets S, Sanchis D, Alvarez B, Ricquier D, Lopez-Soriano FJ and Argiles JM: In the rat, tumor necrosis factor alpha administration results in an increase in both UCP2 and UCP3 mRNAs in skeletal muscle: a possible mechanism for cytokine-induced thermogenesis? FEBS Lett 440: 348-350, 1998.
36. Mattiasson G, Shamloo M, Gido G, *et al*: Uncoupling protein-2 prevents neuronal death and diminishes brain dysfunction after stroke and brain trauma. Nat Med 9: 1062-1068, 2003.
37. Yasuhara S, Perez ME, Kanakubo E, *et al*: Skeletal muscle apoptosis after burns is associated with activation of proapoptotic signals. Am J Physiol Endocrinol Metab 279: E1114-E1121, 2000.
38. Maass DL, Hybki DP, White J and Horton JW: The time course of cardiac NF-kappaB activation and TNF-alpha secretion by cardiac myocytes after burn injury: contribution to burn-related cardiac contractile dysfunction. Shock 17: 293-299, 2002.
39. Yu YM, Tompkins RG, Ryan CM and Young VR: The metabolic basis of the increase of the increase in energy expenditure in severely burned patients. JPEN J Parenter Enteral Nutr 23: 160-168, 1999.
40. Cline GW, Vidal-Puig AJ, Dufour S, Cadman KS, Lowell BB, and Shulman GI: *In vivo* effects of uncoupling protein-3 gene disruption on mitochondrial energy metabolism. J Biol Chem 276: 20240-20244, 2001.
41. Petersen KF, Befroy D, Dufour S, *et al*: Mitochondrial dysfunction in the elderly: possible role in insulin resistance. Science 300: 1140-1142, 2003.
42. Petersen KF, Dufour S, Befroy D, Garcia R and Shulman GI: Impaired mitochondrial activity in the insulin-resistant offspring of patients with type 2 diabetes. N Engl J Med 350: 664-671, 2004.
43. Thompson MP and Kim D: Links between fatty acids and expression of UCP2 and UCP3 mRNAs. FEBS Lett 568: 4-9, 2004.
44. Ikezu T, Okamoto T, Yonezawa K, Tompkins RG, and Martyn JA: Analysis of thermal injury-induced insulin resistance in rodents. Implication of postreceptor mechanisms. J Biol Chem 272: 25289-25295, 1997.
45. Kennedy JE, Ter Haar GR and Cranston D: High intensity focused ultrasound: surgery of the future? Br J Radiol 76: 590-599, 2003.